JTE
HCMUTE
ISSN: 2615-9740

JOURNAL OF TECHNICAL EDUCATION SCIENCE
Ho Chi Minh City University of Technology and Education
Website: https://jte.edu.vn
Email: jte@hcmute.edu.vn

Design Decoupling Control and Wavelet Type-2 Fuzzy Brain Imitated Neural Network (WT2FBINN) for rotational actuator (TORA) System

Duc-Hung Pham[1], Van-Phong Vu[2*]
[1]*Faculty of Electrical and Electronic Engineering, Hung Yen University of Technology and Education, Vietnam*
[2]*Department of Automatic Control, Ho Chi Minh City University of Technology and Education, Vietnam*

[*]Corresponding author. *Email: phongvv@hcmute.edu.vn*

ARTICLE INFO

Received: 04/03/2023
Revised: 18/04/2023
Accepted: 10/05/2023
Published: 28/08/2023

KEYWORDS

Wavelet type-2 fuzzy system;
Brain imitated neural network;
TORA systems;
Decoupling control.

ABSTRACT

In this article, a new wavelet type-2 fuzzy brain imitated neural network (WT2FBINN) is presented for nonlinear system decoupling control. A sliding mode control combined with a decoupling control is illustrated. The control system comprises of a proposed WT2FBINN and a robust controller. The WT2FBINN is used as the main controller to approach an ideal controller to achieve desired control performance, and the robust controller is used to eliminate the approximation error to achieve system stability. The WT2FBINN contains a wavelet type-2 fuzzy system and a brain imitated neural network. The parameters of the proposed WT2FBINN can be updated by the gradient descent method. Then, the WIT2FBINN is applied to control underactuated systems, such as a rotational actuator (TORA) system. Finally, simulation results have validated the effectiveness of the proposed control approach. A comparison to a recently developed method is useful for better illustrating the benefits of the proposed method.

Doi: https://doi.org/10.54644/jte.78A.2023.1358

1. Introduction

An underactuated mechanical system (UMS) is one that has fewer independent control actuators than degrees of freedom (DOF) to be controlled. This class of systems is the subject of active scientific research due to its wide application in various disciplines [1]. Examples of such systems include mobile robots, spacecraft, underwater vehicles, surface ships, helicopters, space robots, and underpowered manipulators [2–5]. Till now, several control techniques have been applied for UMS control, such as sliding mode control (SMC) and some intelligent control algorithms. Sliding mode control has been proposed as an approach for controlling systems with nonlinearities, uncertain dynamics, and bounded input disturbances [6, 7]. When a mechanical system has fewer independent control actuators than the number of controllable DOF, it is underactuated. Due to its wide applicability, this class of systems is the focus of current scientific investigation [1]. Consequently, the control of unactuated mechanical systems (UMS) is currently one of the most rapidly expanding subfields of control engineering. A rotational actuator (TORA) system is also known as an under-actuated mechanical system (UMS) [1]. Due to the TORA system's nonlinear and time-varying behavior, it is difficult to develop an accurate model for the purposes of designing a model-based controller. It can handle both time-varying and nonlinear uncertainty behaviors and can dynamically adjust the control rule's parameters.

Sliding-mode control (SMC) is a technique for regulating nonlinear systems with unknown dynamics and limited input disturbances [1, 2, 3, 4]. Although SMC performs well for coupled second-order systems, its performance for coupled fourth-order systems is debatable. The technique of decoupled sliding mode control (DSMC) has been proposed in order to regulate fourth-order systems for which a single control input is insufficient. In this process, sliding mode control is decoupled. [5]. It enables the subdivision of a set of fourth-order systems into two second-order subsystems, each of which can have a control objective expressed in terms of a sliding surface. The fact that a set of fourth-order systems can be partitioned into two sets of second-order systems [6, 7] makes this possible. DSMC has the significant effect of integrating the second subsystem into the first by incorporating a two-stage decoupling strategy and a sub-slip surface-derived intermediate variable. This is accomplished by

introducing a new variable at the intermediate stage. [5, 6, 7]. Given the difficulty in analyzing nonlinear under mechanical systems (UMSs), neither SMC nor DSMC proves useful as a problem-solving method. To address these issues, Lucas et al. [8] propose a brain imitated neural network (BINN) model that takes cues from the human brain. An intelligent controller, the BINN can change its parameters on the fly [2, 9-11].

Nonlinear systems with a single input and a single sub control of fourth order are the focus of this study because of the potential for decoupling control. Two second-order sliding surfaces can have their decoupling surface defined by introducing an intermediate variable. Nonlinear systems with a single input and a single fourth-order subcontrol are the focus of this work as we study their decoupling control. The decoupling sliding surface between two second-order sliding surfaces can be defined by introducing an intermediate variable. The decoupling control can be achieved with a proposed wavelet type-2 fuzzy brain imitated neural network (WT2FBINN). The proposed control system is based on a WT2FBINN and a robust compensator. The WT2FBINN is the primary controller used to approximate an ideal controller, and the robust compensator is used to eliminate approximation errors and ensure system stability. By applying the proposed control algorithm to the control of a TORA system, we show that it is effective. The simulations approve the advantage of the proposed control method completed competing control methods.

2. Problem Formulation

Considering the expression below for an under actuated nonlinear system [1]:

$$\begin{cases} \dot{\chi}_1 = \chi_2 \\ \dot{\chi}_2 = \Psi_1 + b_1(\chi_1, \chi_2)u + \rho_1 \\ \dot{\chi}_3 = \chi_4 \\ \dot{\chi}_4 = \Psi_2 + b_2(\chi_1, \chi_2)u + \rho_2 \end{cases} \quad (1)$$

where b_1, b_2 Ψ_1, Ψ_2 stand for nonlinear functions, ρ_1, ρ_2 stand for matched disturbances, u stands for control input, and $\chi = [\chi_1\ \chi_2\ \chi_3\ \chi_4]^T$ stands for state vector. Following is a description of tracking errors:

$$e_i = \chi_{id} - \chi_i \text{ with } i = 1,2,3,4 \quad (2)$$

where χ_{id} stands for goal values. Using sliding surface we can reduce the number of errors e_1, e_2, e_3, e_4 to two variables s_1, s_2 with κ_1, κ_2 as coefficients, as follows.

$$s_1 = \kappa_1(e_1 - z) + e_2 \quad (3)$$

$$s_2 = \kappa_2 e_3 + e_4 \quad (4)$$

ζ can be calculated as follows

$$\zeta = \text{saturaion}(\frac{s_2}{\Phi_z})\zeta_\kappa, \quad 0 < \zeta_\kappa < 1 \quad (5)$$

where Φ_κ is the boundary space of s_2. In addition, the saturation(.) function is defined as

$$\text{saturation}(\frac{s_2}{\Phi_\kappa}) = \begin{cases} \frac{s_2}{\Phi_\kappa}, & \text{when } \left|\frac{s_2}{\Phi_\kappa}\right| < 1 \\ \text{sgn}(\frac{s_2}{\Phi_\kappa}), & \text{when } \left|\frac{s_2}{\Phi_\kappa}\right| \geq 1 \end{cases} \quad (6)$$

The ideal controller shown below can be derived from and is capable of stabilizing the system (1).

$$u_{\text{IDEAL}} = b_1^{-1}\left(-\kappa_1\chi_2 - \kappa_1\dot{z} - \Psi_1 + \kappa_1\dot{\chi}_{1d} + \dot{\chi}_{2d} - \rho_1\right) \quad (7)$$

The ideal controller in equation (7) is currently unavailable due to a technical issue, because the nonlinear function Ψ_1 and the disturbance ρ_1 cannot be measured exactly. As a good approximation to the ideal controller, we propose a wavelet type-2 fuzzy brain imitated neural network (WT2FBINN). in this work.

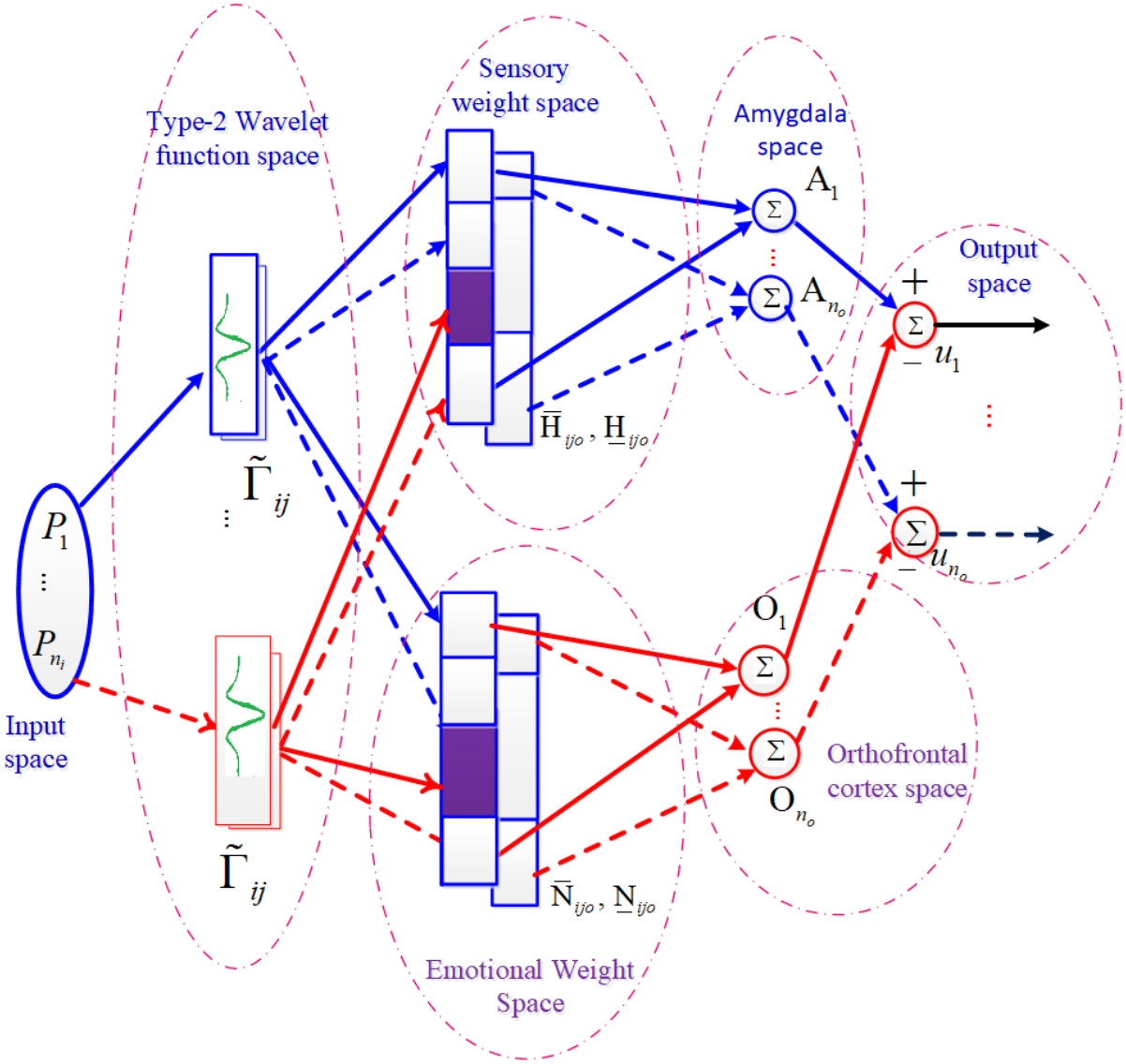

Figure 1. *The design of WT2FBINN*

3. WT2FBINN controller

The examples below illustrate fuzzy inference rules:

$$\text{If } P_1 \text{ is } \Gamma_{1j} \text{ and } P_2 \text{ is } \Gamma_{2j},\ldots, \text{ and } P_{n_i} \text{ is } \Gamma_{n_i j} \quad \text{then } O_o = N_{ijo} \text{ and } A_o = H_{ijo} \tag{8}$$

where n_i, n_j, and n_o $(j=1,2...,n_j,\ o=1,2...,n_o)$ stand respectively for input dimension, layer dimension and output dimension; Γ_{ij} stands for wavelet type-2 function; O_o and A_o stand respectively for *o*-th output of orbitofrontal cortex and amygdala.

Figure 1 depicts the WT2FBINN's internal structure, which contains five spaces: input space, wavelet type-2 function space, emotion and sensory weight space, orbitofrontal cortex and amygdala space, and output space.

1. Input space: $P = \left[P_1, P_2,...,P_{n_i}\right] \in \Re^{n_i}$

2. Wavelet type-2 function space

A wavelet type-2 function can be defined as

$$\tilde{\Gamma}_{ij} = \frac{-(P_i - m_{ij})}{\tilde{v}_{ij}} e^{\frac{-(P_i - m_{ij})^2}{2\tilde{v}_{ij}^2}} \tag{9}$$

where $\overline{v}_{ij}$, $\underline{v}_{ij}$ stand for the upper and lower values of $\tilde{v}_{ij}$. $\tilde{v}_{ij} = [\overline{v}_{ij} \ \underline{v}_{ij}]$, m_{ij} stand respectively for variance and mean of wavelet type-2 function.

3. Emotion and sensory weight space

Both the upper and lower weights of the sensory system are represented by $\overline{\gamma}_{ijo}$ and $\underline{\gamma}_{ijo}$ respectively. The upper and lower weights of emotional experience are represented by $\overline{\mu}_{ijo}$ and $\underline{\mu}_{ijo}$, respectively.

4. Orbitofrontal cortex and amygdala space

orbitofrontal cortex and amygdala space can be calculated as follows, by way to the kernel, wavelet type-2 function and weight.

$$\mathrm{A}_o = \frac{1}{2}\left(\frac{\sum_{i=1}^{n_i}\sum_{j=1}^{n_j} \Gamma_{ij}^r \overline{\mathrm{H}}_{ijo}}{\sum_{i=1}^{n_i}\sum_{j=1}^{n_j} \Gamma_{ij}^r} + \frac{\sum_{i=1}^{n_i}\sum_{j=1}^{n_j} \Gamma_{ij}^l \underline{\mathrm{H}}_{ijo}}{\sum_{i=1}^{n_i}\sum_{j=1}^{n_j} \Gamma_{ij}^l} \right) \tag{10}$$

$$\mathrm{O}_o = \frac{1}{2}\left(\frac{\sum_{i=1}^{n_i}\sum_{j=1}^{n_j} \Gamma_{ij}^r \overline{\mathrm{N}}_{ijo}}{\sum_{i=1}^{n_i}\sum_{j=1}^{n_j} \Gamma_{ij}^r} + \frac{\sum_{i=1}^{n_i}\sum_{j=1}^{n_j} \Gamma_{ij}^l \underline{\mathrm{N}}_{ijo}}{\sum_{i=1}^{n_i}\sum_{j=1}^{n_j} \Gamma_{ij}^l} \right) \tag{11}$$

One of the many things that the Karnik-Mendel [13] algorithm can calculate is type-2 to type-1 reduction.

$$\Gamma_{ij}^l = \begin{cases} \underline{\Gamma}_{ij}, \ j > L_{\text{eft}} \\ \overline{\Gamma}_{ij}, \ j \le L_{\text{eft}} \end{cases} \tag{12}$$

$$\Gamma_{ij}^r = \begin{cases} \overline{\Gamma}_{ij}, \ j > R_{\text{ight}} \\ \underline{\Gamma}_{ij}, \ j \le R_{\text{ight}} \end{cases} \tag{13}$$

where R_{ight} and L_{eft} denote right switching point and left switching point.

5. Output space

The *o*-th ouput of proposed controller can be defined as follows

$$u_o \equiv \mathrm{A}_o - \mathrm{O}_o \tag{14}$$

Then, total ouput of the WT2FBINN is calculated as follows

$$u_{\text{WT2FBINN}} = \sum_{o=1}^{n_o} u_o \tag{15}$$

As part of WT2FBINN parameters ($\overline{\mathrm{N}}_{ijo}, \underline{\mathrm{N}}_{ijo}, \overline{\mathrm{H}}_{ijo}, \underline{\mathrm{H}}_{ijo}$), the upper and lower weights of the amygdala and orbitofrontal cortex are comprised. The updating laws for all parameters can be calculated as follows.

$$\Delta\overline{\mathrm{N}}_{ijo}(t) = \eta_{\overline{\mathrm{N}}}(\overline{S}_{ij}(u_o(t) - Rw_o(t))) \tag{16}$$

$$\Delta\underline{\mathrm{N}}_{ijo}(t) = \eta_{\underline{\mathrm{N}}}(\underline{\Gamma}_{ij}(u_o(t) - Rw_o(t))) \tag{17}$$

$$\overline{\mathrm{N}}_{ijo}(t+1) = \overline{\mathrm{N}}_{ijo}(t) + \Delta\overline{\mathrm{N}}_{ijo}(t) \tag{18}$$

$$\underline{\mathrm{N}}_{ijo}(t+1) = \underline{\mathrm{N}}_{ijo}(t) + \Delta\underline{\mathrm{N}}_{ijo}(t) \tag{19}$$

$$\Delta\bar{\mathrm{H}}_{ijo}(t) = \xi_{\bar{\mathrm{H}}}.(\bar{\Gamma}_{ij}.\max(0, Rw_o(t) - \mathrm{A}_o(t)) \quad (20)$$

$$\Delta\underline{\mathrm{H}}_{ijo}(t) = \eta_{\underline{\mathrm{H}}}.(\underline{\Gamma}_{ij}.\max(0, Rw_o(t) - \mathrm{A}_o(t)) \quad (21)$$

$$\bar{\mathrm{H}}_{ijo}(t+1) = \bar{\mathrm{H}}_{ijo}(t) + \Delta\bar{\mathrm{H}}_{ijo}(t) \quad (22)$$

$$\underline{\Gamma}_{ijo}(t+1) = \underline{\Gamma}_{ijo}(t) + \Delta\underline{\Gamma}_{ijo}(t) \quad (23)$$

where $\eta_{\bar{\mathrm{H}}}, \eta_{\underline{\mathrm{H}}}, \eta_{\bar{\mathrm{N}}}$, and $\eta_{\underline{\mathrm{N}}}$ values denote the learning rates, Rw_o denotes a desired value. Choosing a cost function as follows.

$$V(s_1) = \frac{1}{2}s_1^2 \quad (24)$$

Taking the derivative of equation (24), gets

$$\dot{V} = s_1\dot{s}_1 \quad (25)$$

The following revised laws were discovered by using the gradient descent method.

$$\Delta m_{ij} = -\eta_m.\frac{\partial\dot{V}}{\partial m_{ij}} = -\eta_m\underbrace{(\frac{\partial(s_1\dot{s}_1)}{\partial u_{\mathrm{WT2FBINN}}})}_{=b_1s_1}\underbrace{(\frac{\partial u_{\mathrm{WT2FBINN}}}{\partial u_o})}_{=1}\frac{\partial u_o}{\partial m_{ij}} =$$

$$= \eta_m b_1 s_1\left((\underline{\gamma}_{ijo} - \underline{\mu}_{ijo}).e^{(\frac{-\underline{\Upsilon}_{ij}^2}{2})}.\left(2-\underline{\Upsilon}_{ij}^2\right).\frac{\underline{\Upsilon}_{ij}}{\underline{v}_{ij}} + (\bar{\gamma}_{ijo} - \bar{\mu}_{ijo}).e^{(\frac{-\bar{\Upsilon}_{ij}}{2})}.\left(2-\bar{\Upsilon}_{ij}^2\right)\frac{\bar{\Upsilon}_{ij}}{\bar{v}_{ij}}\right) \quad (26)$$

$$\Delta\underline{v}_{ij} = -\eta_{\underline{v}}.\frac{\partial\dot{V}}{\partial\underline{v}_{ij}} = -\eta_{\underline{v}}.\frac{\partial(s_1\dot{s}_1)}{\partial u_{\mathrm{WT2FBINN}}}.\frac{\partial u_{\mathrm{WT2FBINN}}}{\partial u_o}.\frac{\partial u_o}{\partial\underline{v}_{ij}} = \eta_{\underline{v}}.b_1.s_1.\underline{\psi}_{ij}.\sum_{o=1}^{n_o}(\underline{\gamma}_{ijo} - \underline{\mu}_{ijo}).\frac{(\underline{\Upsilon}_{ij}^2 - 2)}{\underline{v}_{ij}} \quad (27)$$

$$\Delta\bar{v}_{ij} = -\eta_{\bar{v}}.\frac{\partial\dot{V}}{\partial\bar{v}_{ij}} = -\eta_{\bar{v}}.\frac{\partial(s_1\dot{s}_1)}{\partial u_{\mathrm{WT2FBEC}}}.\frac{\partial u_{\mathrm{WT2FBEC}}}{\partial u_o}.\frac{\partial u_o}{\partial\bar{v}_{ij}} = \eta_{\bar{v}}.b_1.s_1.\sum_{o=1}^{n_o}(\bar{\gamma}_{ijo} - \bar{\mu}_{ijo}).\bar{\psi}_{ij}.\frac{(\bar{\Upsilon}_{ij}^2 - 2)}{\bar{v}_{ij}} \quad (28)$$

where $\eta_m, \eta_{\underline{v}}$, and $\eta_{\bar{v}}$ denote learning rates with small values. The illustration of the proposed control system is shown in Fig. 2 as below.

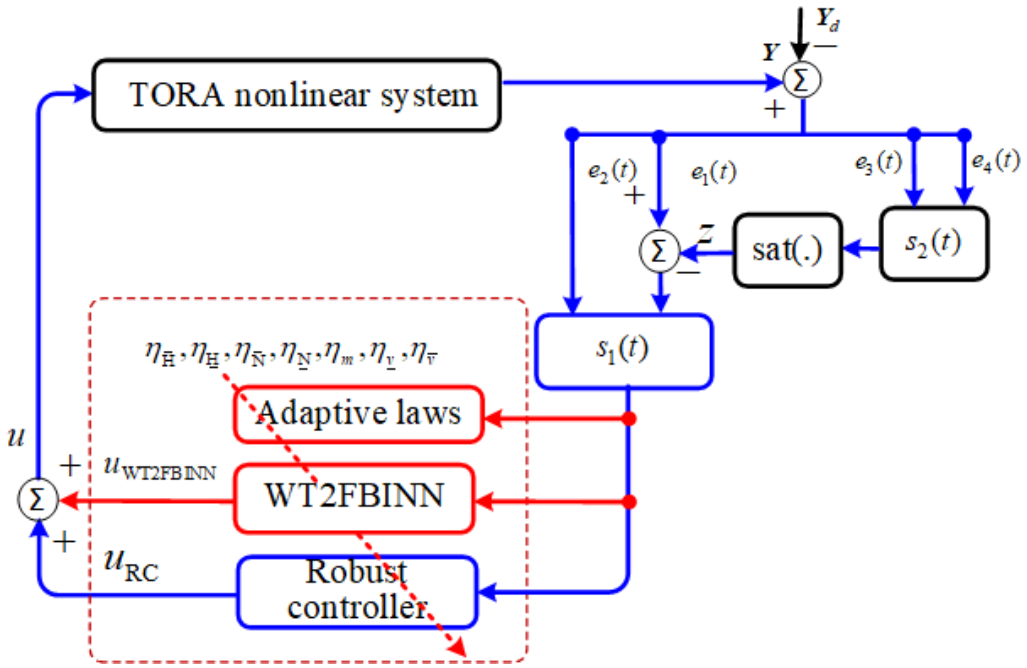

Figure 2. *Proposed control system diagram*

Equation (1) describes a TORA nonlinear system. If the WT2FBINN and online factor tuning algorithms described in equations (16)-(28) are used in the design of the control system via equation (15) and the robust compensator controller, the stability of the control system can be guaranteed. This is possible due to the robust compensator of the controller. Choosing a cost function in the following.

$$V_1 = \frac{1}{2} s_1^2 \tag{29}$$

$$\Rightarrow \dot{V}_1 = s_1 \dot{s}_1 \tag{30}$$

If approximation error is constant, the ideal controller is the sum of our method and the approximation error.

$$\Xi = u_{\text{IDEAL}} - u_{\text{WT2FBINN}} \tag{31}$$

where Ξ is the approximation error. A control system can be designed to compensate for approximation error as follows:

$$u = u_{\text{WT2FBINN}} + u_{\text{RC}} \tag{32}$$

where u_{RC} denotes robust compensation controller. Figure 2 depicts the control system diagram. From (1), gets:

$$\dot{y}_2 = \Psi_1 + b_1(u_{\text{WT2FBINN}} + u_{\text{RC}} - u_{\text{IDEAL}}) + b_1 u_{\text{IDEAL}} + \rho_1 \tag{33}$$

By substituting u_{IDEAL} in equation (7) for equation (33), we get

$$\dot{y}_2 = b_1(u_{\text{WT2FBINN}} + u_{\text{RC}} - u_{\text{IDEAL}}) + (\Psi_1 - \kappa_1 x_2 - \kappa_1 \dot{z} - g_1 + \kappa_1 \dot{y}_{1d} + \dot{y}_{2d}) \tag{34}$$

Taking the derivative of equation (3), gets

$$\dot{s}_1 = \kappa_1(\dot{e}_1 - \dot{z}) + \dot{e}_2 = \kappa_1(\dot{y}_{1d} - \dot{y}_1 - \dot{z}) + \dot{y}_{2d} - \dot{y}_2 \tag{35}$$

Substituting $\dot{y}_2$ from equation (33) into (35), attains

$$\dot{s}_1 = b_1.\left(u_{\text{IDEAL}} - u_{\text{WT2FBINN}} - u_{\text{RC}}\right) \tag{35}$$

The robust compensation controller is selected as follows

$$u_{\text{RC}} = (2\Upsilon^2)^{-1}(\Upsilon^2 + \text{I})\, s_1(t) \tag{36}$$

where $\Upsilon = diag(r_i)$ and I is an unity matrix. If the control system (15) is provided for the feedback scheme depicted in Figure 2, along with the proposed technique and the robust compensator (35), then the robust constancy in (36) is certain [2].

3. Simulation results

The parameters of TORA system are described in Table 1 as follows.

Table 1. *TORA parameters meaning*

Parameters	Meaning
r	the radius of rotation
k	the stiffness of the linear spring
θ	the rotational angle
ρ	the disturbance force acting on the cart
y_c	translational position
m_ω	the rotor mass
I	the moment of inertia of the eccentric mass

M	the total mass of the rotor and car

A TORA system are shown in Figure 3. While nonlinearity in and of itself presents challenges, the TORA system also benefits from a physically meaningful concept of energy storage. In order to demonstrate the absence of gravitational influence, a DC motor drives a horizontally rotating proof mass that is attached to a translating cart. A initially stiff spring and DC motor torque are the only things keeping the cart in motion.

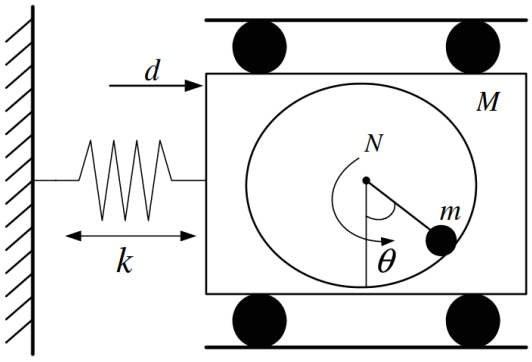

Figure 3. *Structure of the TORA system*

By adjusting the torque input, we wish to minimize oscillations in the proof mass in this problem [1]. This is the movement of oscillations:

$$\begin{aligned}(M+m_\omega)\ddot{y}_c + m_\omega r(\ddot{\theta} - \dot{\theta}^2\sin\theta) + ky_c &= \rho \\ (I+m_\omega r^2)\dot{\theta}^2 + m_\omega \ddot{y}_c r\cos\theta &= U\end{aligned} \tag{37}$$

We can rewrite (44) using a normalization transformation in the space of state variables as:

$$\begin{aligned}&\dot{\chi}_1 = \chi_2,\ \dot{\chi}_2 = -\chi_1 + \delta\sin(\chi_3) + \rho \\ &\dot{\chi}_3 = \chi_4,\ \dot{\chi}_4 = -\frac{\delta\cos\theta}{1-\delta^2\cos^2(\chi_3)}(\chi_1 - \delta(1+\chi_4^2)\sin(\chi_3) - \rho) + \frac{1}{1-\delta^2\cos^2(\chi_3)}u\end{aligned} \tag{38}$$

where $\chi_1, \chi_2, \chi_3, \chi_4$ are respectively cart position, cart velocity, rotor angle, and rotor angular velocity; $0 < \delta < 1$, u is control input. ρ represents disturbance and. Assuming $\delta = 0.1$. Following are explanations of the following terms:

$$s_1 = c_1(\theta - z) + \dot{\theta} = c_1(\chi_1 - z) + \chi_2,\ s_2 = c_2\chi + \dot{\chi} = c_2\chi_3 + \chi_4 \tag{39}$$

$$z = \text{sat}(s_2 / \Phi_z)\cdot Z_{\text{upper}},\qquad 0 < Z_{\text{upper}} < 1 \tag{40}$$

Parameters are used in the simulation are chosen as follows

$\Phi_z = 10,\ \ c_1 = 2,\ c_2 = 3,\ Z_{\text{upper}} = 0.8,\ \ |\rho| \le 0.04,\ \ y_1 = 0, y_2 = 1,\ \theta = y_3 = 0$. The control parameter diagram is depicted in Figure 4 below. The parameters of the proposed controller are shown in Table 2 as below.

Table 2. *Initial parameters of the proposed method*

Parameters	Values
$\eta_{\bar{H}}, \eta_{\underline{H}}, \eta_{\bar{N}}, \eta_{\underline{N}}, \eta_m, \eta_{\underline{v}}, \eta_{\bar{v}}$	0.002
$\underline{v}$	0.4
$\bar{v}$	0.5
m	0.03

$\bar{H}_{ijo}$	0.03
$\underline{N}_{ijo}$	0.002
$\bar{N}_{ijo}$	0.025
$\underline{H}_{ijo}$	0.02

Figures 5-7 show that the WT2FBINN control method outperforms cerebellar model articulation control (CMAC) [12, 13], fuzzy brain imitated neural network (FBINN) [14], and fuzzy brain emotional cerebellar model controller (FBECMAC) [2] in terms of settling time, overshoot performance, and robustness. Furthermore, when the root mean square error (RMSE) for the TORA system is calculated, the RMSE of WT2FBINN is less than that of the cerebellar model articulation control (CMAC) [12, 13] 5.671 times, fuzzy brain imitated neural network (FBINN) [14] 5.503 times, and FBECMAC [2] 3.83 times. In conclusion, the proposed WT2FBINN method outperforms the CMAC, FBINN and FBECMAC method. The fuzzy brain emotional cerebellar model controller (FBECMAC) should be used in comparison to the proposed controller because it is structured similarly to WT2FBINN, with the exception that FBECMAC uses type-1 fuzzy systems and WT2FBINN uses type-2 fuzzy systems. Furthermore, the FBECMAC suite has been shown to be effective for nonlinear systems [2].

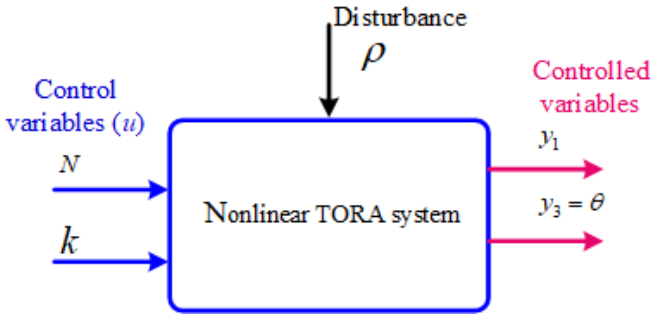

Figure 4. *The control parameters diagram*

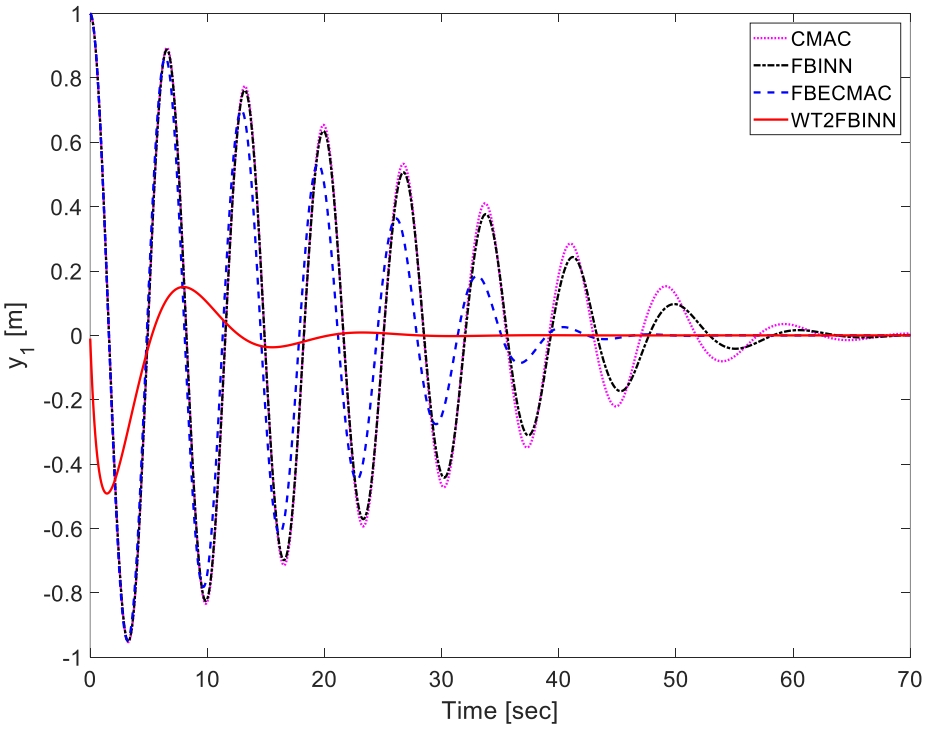

Figure 5. *The outcomes of TORA's controlled testing for* y_1

JTE
HCMUTE
ISSN: 2615-9740

JOURNAL OF TECHNICAL EDUCATION SCIENCE
Ho Chi Minh City University of Technology and Education
Website: https://jte.edu.vn
Email: jte@hcmute.edu.vn

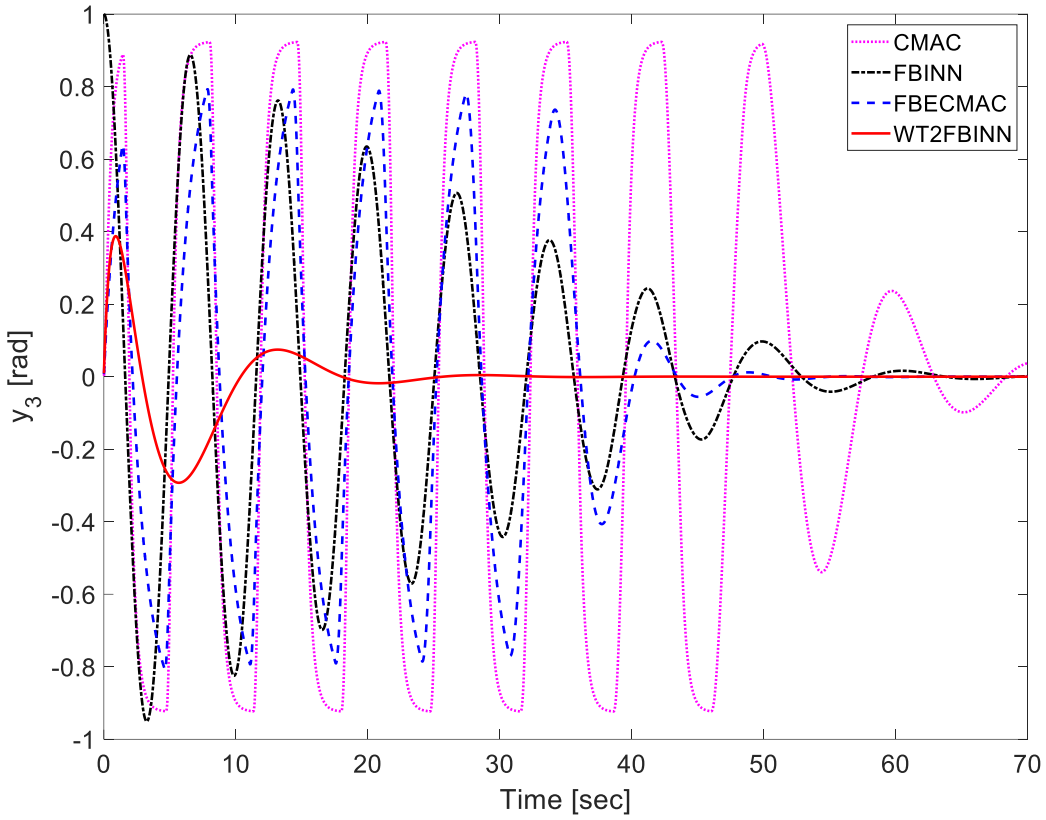

Figure 6. *The outcomes of TORA's controlled testing for* y_3

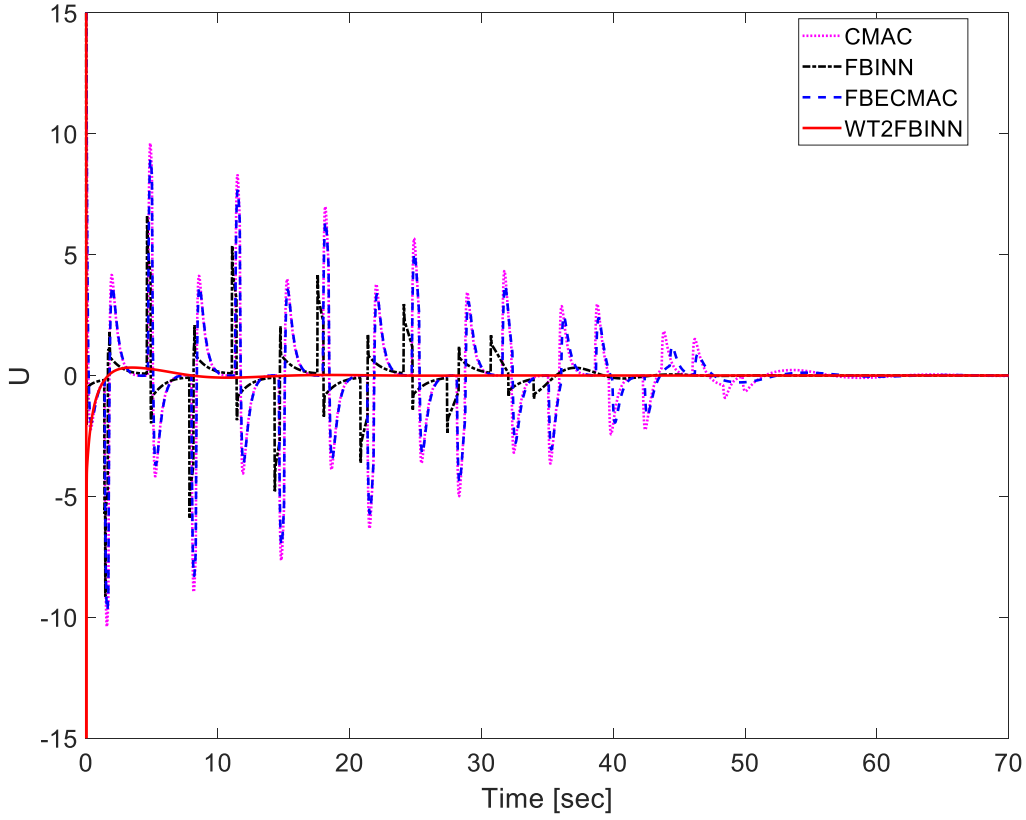

Figure 7. *The outcomes of TORA's controlled testing for u*

Table 3. *RMSE comparisons of WT2FBINN, CMAC, FBINN and FBECMAC*

Method	RMSE of y_3	RMSE of y_1	Average_RMSE
CMAC [12, 13]	0.5620	0.3102	0.4361
FBINN [14]	0.5442	0.3021	0.4232
FBECMAC [2]	0.4351	0.1534	0.2943
WT2FBINN	0.0714	0.0823	0.0769

4. Conclusions

A WT2FBINN and a robust controller have been used to propose a decoupled sliding mode control of single-input, four-order nonlinear systems that are inactive. The proposed method is compared with other control techniques in a simulation study for the TORA system. The simulation results show that the proposed control system is effective. The designed controller is effective in tracking with small errors and shows fast convergence. However, some of the parameters of the designed controller should be determined by trial and error. In the future, an auto-optimization algorithm such as Modified Grey Wolf Optimizer (MGWO) could be used to select the optimal learning rates for the proposed WT2FBINN-based control system to improve the learning ability of the parameters and reduce the control error. Since the developed WT2FBINN is a multiple-output network, the proposed approach is also applicable to multiple-input and multiple-output systems.

REFERENCES

[1] L. C. Hung and H. Y. Chung, "Decoupled Sliding-Mode with Fuzzy-Neural Network Controller for Nonlinear Systems," *International Journal of Approximate Reasoning*, vol. 46, no. 1, pp. 74-97, 2007.

[2] G., -L. Guo, C. -M. Lin, H. -Y. Cho, D. -H. Pham, T. -T. Huynh, and F. Chao. "Decoupled sliding mode control of underactuated nonlinear systems using a fuzzy brain emotional cerebellar model control system," *International Journal of Fuzzy Systems*, pp. 1-14, 2022.

[3] J. Huang, S. Ri, T. Fukuda and Y. Wang, "A disturbance observer based sliding mode control for a class of underactuated robotic system with mismatched uncertainties," *IEEE Transaction on Automatic Control*, vol. 64, no. 6, pp. 2480-2486, 2019.

[4] C. M. Lin, and Y. J. Mon, "Decoupling control by hierarchical fuzzy sliding-mode controller," *IEEE Transactions on Control Systems Technology*, vol. 13, no. 4, pp. 593-598, 2005.

[5] C.-L. Huang, C.-C. Chiang and Y.-W. Yeh, "Adaptive fuzzy hierarchical sliding-mode control for the trajectory tracking of uncertain underactuated nonlinear dynamic systems," *IEEE Transaction on Fuzzy Sysatems*, vol. 22, no. 2, pp. 286-299, 2014.

[6] S. Yang, Z. Li, R. Cui and B. Xu, "Neural network-based motion control of an underactuated wheeled inverted pendulum model," IEEE Transaction on Neural Network and Learning Systems, vol. 25, no. 11, pp. 2004-2016, 2014.

[7] T. Yang, H. Chen, N. Sun, and Y. Fang,"Adaptive neural network output feedback control of uncertain underactuated systems with actuated and unactuated state constraints," *IEEE Transactions on Systems, Man, and Cybernetics: Systems*, 2021, doi: 10.1109/TSMC.2021.3131843.

[8] C. Lucas, D. Shahmirzadi, and N. Sheikholeslami, "Introducing BELBIC: Brain emotional learning based intelligent controller," *International Journal of Intelligent Automation and Soft Computing*, vol. 10, no. 1, pp. 11-21, 2004.

[9] D. -H. Pham, C. -M. Lin, V. N. Giap, T. -T. Huynh and H. -Y. Cho, "Wavelet Interval Type-2 Takagi-Kang-Sugeno Hybrid Controller for Time-Series Prediction and Chaotic Synchronization," in *IEEE Access*, vol. 10, pp. 104313-104327, 2022.

[10] C.-M. Lin, D.-H. Pham, and T.-T. Huynh, "Synchronization of chaotic system using a brain-imitated neural network controller and its applications for secure communications," *IEEE Access*, vol. 9, pp. 75923-75944, 2021.

[11] C. -M. Lin, D. -H. Pham and T. -T. Huynh, "Encryption and Decryption of Audio Signal and Image Secure Communications Using Chaotic System Synchronization Control by TSK Fuzzy Brain Emotional Learning Controllers," *IEEE Transactions on Cybernetics*, vol. 52, no. 12, pp. 13684-13698, 2022.

[12] T. -T. Huynh, D. -H. Pham and N. T. Son, "A Brain Emotional Fuzzy CMAC for Chaos Synchronization and Communication," 2022 6th International Conference on Green Technology and Sustainable Development (GTSD), Nha Trang City, Vietnam, pp. 131-134, 2022. doi: 10.1109/GTSD54989.2022.9989169.

[13] T. -T. Huynh, D. -H. Pham and N. T. Son, "Image Secure Communication Using BELC-CMAC and Chaos Synchronization," 2022 6th International Conference on Green Technology and Sustainable Development (GTSD), Nha Trang City, Vietnam, 2022, pp. 135-139, doi: 10.1109/GTSD54989.2022.9988766.

[14] D. -H. Pham, T. -T. Huynh and C. -M. Lin, "Fault-Tolerant Control for Robotic Systems Using a Wavelet Type-2 Fuzzy Brain Emotional Learning Controller and a TOPSIS-Based Self-organizing Algorithm," International journal of fuzzy system, 2023. https://doi.org/10.1007/s40815-023-01516-y

Pham Duc Hung was born in Hung Yen Province, Vietnam, in 1983. He received the B.S. degree in Automatic Control from Hanoi University of Science and Technology, Vietnam, in 2006, the M.S. degree in Automation from Hanoi University of Science and Technology, Vietnam, in 2011, and he received Ph.D. degree in the Department of Electrical Engineering, Yuan Ze University, Chung-Li, Taiwan, in 2022. He is also a Lecturer with Faculty Electrical and Electronic, Hung Yen University of technical and education, Vietnam. His research interests include fuzzy logic control, neural network, cerebellar model articulation controller, brain emotional learning-based intelligent controller, fault tolerant control, secure communication. Email: *duchung.pham@utehy.edu.vn*

Vu Van Phong received the B.S. degree in the Department of Automatic Control from Hanoi University of Sciences and Technology, Hanoi, Vietnam in 2007; and M.S. degree in the Department of Electrical Engineering from Southern Taiwan University of Sciences and Technology, Tainan, Taiwan in 2010. Moreover, he received the Ph.D. degree in the Department of Electrical Engineering from National Central University, Zhongli, Taiwan, in 2017. Dr. Vu is currently a Lecturer with the Ho Chi Minh City University of Education and Technology, Ho Chi Minh City. His research interests include the fuzzy system, intelligent control, observer and controller design for the uncertain system, polynomial system, fault estimation, and large-scale system. Email: *phongvv@hcmute.edu.vn*